Naranjo et al. Journal of Applied Volcanology (2016) 5:8
DOI 10.1186/s13617-016-0048-z

Journal of Applied Volcanology

RESEARCH Open Access

Mapping and measuring lava volumes from 2002 to 2009 at El Reventador Volcano, Ecuador, from field measurements and satellite remote sensing

M. Fernanda Naranjo[1*], Susanna K. Ebmeier[2*], Silvia Vallejo[1], Patricio Ramón[1], Patricia Mothes[1], Juliet Biggs[2] and Francisco Herrera[3]

Abstract

Estimates of lava volume, and thus effusion rate, are critical for assessing volcanic hazard and are a priority for volcano observatories with responsibility for monitoring. The choice of specific methods used to approximate lava volume depends on both volcanological and practical considerations; in particular, whether field measurements are possible and how often they can be repeated. Volcán El Reventador (Ecuador) is inaccessible, and field measurements can only be made infrequently at a few locations in its caldera. We present both planimetric field and topographic satellite radar-based measurements of lava flow thicknesses and volumes for activity at El Reventador between 2002 and 2009. Lava volumes estimates range from $75 \pm 24 \times 10^6$ m^3 (based on field measurements of flow thickness) to $90 \pm 37 \times 10^6$ m^3 (from satellite radar retrieval of flow thickness), corresponding to time-averaged effusion rates of 9 ± 4 m^3/s and 7 ± 2 m^3/s, respectively. Detailed flow mapping from aerial imagery demonstrate that lava effusion rate was at its peak at the start of each eruption phase and decreased over time. Measurements of lava thickness made from a small set of Synthetic Aperture Radar (SAR) interferograms allowed the retrieval of the shape of the compound lava flow field and show that in 2009 it was subsiding by up to 6 cm/year. Satellite radar measurements thus have the potential to be a valuable supplement to ground-based monitoring at El Reventador and other inaccessible volcanoes.

Keywords: El Reventador volcano, Lava flows, InSAR, Lava effusion rate, Ecuador

Introduction

Effusion rate is critical for assessing lava flow hazards and may be estimated by direct measurements or from repeated mapping of active or newly emplaced lava flows. Over days to weeks, lava flow mapping records the path and advance rate of lava, while over longer timescales, repeat observations of lava flux reflect changes in magma source or in conduit dimensions (e.g., Stasiuk et al. 1993) and, in silicic systems, the likelihood of dome collapse (e.g., Fink and Griffiths 1998). Over the course of an eruption, variations in time-averaged effusion rates may also reveal changes in magma supply (e.g., Poland et al. 2012). Even when measurements are not possible during an eruption, retrospective analysis of lava flows provides an important basis for the development of lava flow hazard maps, especially where the surface area, flow volumes and history of effusive activity can be reconstructed (Cashman et al. 2013).

Lava flows may be mapped directly (e.g., Ryan et al. 2010) or on ground, aerial or satellite photographs and thermal images (eg., Vallejo and Ramón 2012). Flow volumes are estimated by multiplying flow area by measured or estimated mean lava thickness ('planimetric' approach; e.g., Rowland 1996; Stevens et al. 1999). Pre-existing and post-eruption measurements of topography allow a more direct measurement of volume change ('topographic' approach). Satellite imagery specifically suited for constructing a Digital Elevation Model (DEM) has not, until very recently (e.g., TanDem-X, Poland 2014) been acquired regularly and is still not widely available to most volcano observatories. However,

* Correspondence: fnaranjo@igepn.edu.ec; sk.ebmeier@bristol.ac.uk
[1]Instituto Geofísico, Escuela Politécnica Nacional, Quito, Ecuador
[2]School of Earth Sciences, University of Bristol, Bristol BS8 1RJ, UK
Full list of author information is available at the end of the article

DEMs may also be constructed from ground-based and aerial photogrammetry (e.g., Ryan et al. 2010, Diefenbach et al. 2012) or retrieved from differential interferograms (e.g., Ebmeier et al. 2012; Xu and Jónsson 2014).

Here, we compare planimetric and topographic estimates of lava volumes from the eruption of El Reventador, Ecuador from 2002 to 2009.

Background

Volcán El Reventador

El Reventador is a dominantly andesitic stratovolcano on the western edge of the Amazon basin, ~90 km east of Quito (Fig. 1). Work in the 1970s found El Reventador to have had up to twenty eruptive periods since the earliest historical eruption in 1541.[1] These eruptions were characterised by tephra fall, as well as pyroclastic density currents and basaltic to andesitic lava flows. The summit of the volcano hosts a horseshoe-shaped caldera ~4 km across and formed by edifice collapse eastward into the Amazon basin. Historical activity has been centred on a cone with an estimated volume of ~5 km^3 that rises ~1300 m above the caldera floor (Hall 1977). The cone stood 3562 m a.s.l in 1931 (Paz y Miño and y Guerrero 1931), but, following eruptions in the 1970s, was measured at 3450 m. a.s.l. (INECEL 1988).

After nearly three decades of quiescence, El Reventador erupted again on 3 November 2002 marking the start of a prolonged eruptive sequence that continues to this day (as of February 2016). The opening phase was El Reventador's largest explosive historical event (VEI 4) and produced a 17 km high ash column, distributed ash to the west over the Inter-Andean Valley, and generated nine pyroclastic density currents that impacted infrastructure including oil pipelines and roads (Hall et al. 2004) to the east of the volcano. A few days after the initial explosive eruption, the effusion of blocky, andesitic lavas began. Activity at El Reventador from 2002 to date has been dominated by such lava flows.

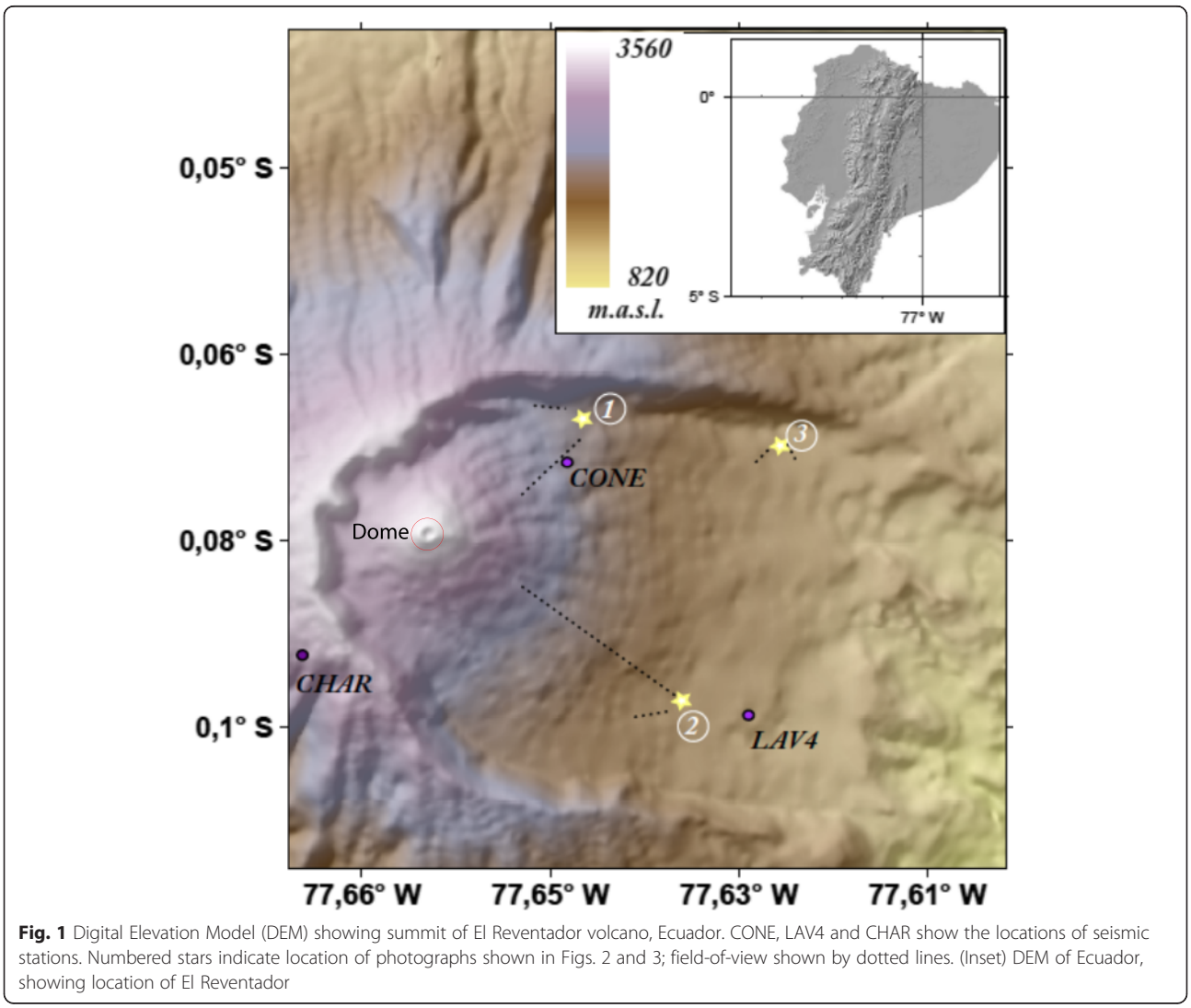

Fig. 1 Digital Elevation Model (DEM) showing summit of El Reventador volcano, Ecuador. CONE, LAV4 and CHAR show the locations of seismic stations. Numbered stars indicate location of photographs shown in Figs. 2 and 3; field-of-view shown by dotted lines. (Inset) DEM of Ecuador, showing location of El Reventador

Observations of eruptions 2002–2009

The *Instituto Geofísico* (IG) at the Escuela Politecnica Nacional conducts field campaigns at El Reventador several times every year, with more than 50 visits to the volcano during 2002–2009. Since the start of the eruption there have been 39 overflights of the volcano. El Reventador is very difficult to access: walking into the caldera through the rainforest requires establishing a base camp, while access by helicopter or light aircraft relies on rare occasions of clear weather and carries the risk of scientists having to walk out of the caldera if the weather changes. El Reventador is covered by cloud the majority of the time – of the 136 ASTER images acquired between 2002 and 2009 only 2 are cloud free over the lava flows (ava.jpl.nasa.gov/ASTER_data.php?id = 1502-01=). Because of these challenges a variety of different monitoring methods were employed to identify periods of active lava effusion between 2002 and 2009. This includes visual and thermal in situ and aerial observations, seismicity, satellite thermal alerts (MODVOLC, HOTSPOT), VAAC alerts and SO_2 emissions from TOMS & OMI (Additional file 1: Figure S1). Monitoring data are summarised in the Additional file 1: Figure S1 and Table 1.

There were four separate phases of eruption between 2002 and 2009 that resulted in at least 17 distinct lava flows. The IG define phases of eruption as being periods when both geophysical indicators (e.g., volcano seismicity, Lees et al. 2008) and emissions (e.g., satellite observations of ash, SO_2 or thermal alerts) are elevated. There was some variation in the character of explosive eruptions and lava flow characteristics between the four eruption phases in 2002–2009, which were separated by periods of relative quiet.

At the onset of the first phase (A, Nov. 2002) there were no seismic stations at El Reventador, and tremor associated with the eruption was first identified from seismic stations at Guagua Pichincha and Cayambe volcanoes. There was high SO_2 emission (60,000 metric tonnes on 3 Nov, falling to ~5000 tones per day by 25 Nov.), significant ash emission and pyroclastic density currents reached as far as the eastern edge of the caldera. Two separate lavas flowed from the small summit crater on the cone and a nearby lateral vent on the southeastern cone and reached a maximum runout distance of 3.7 km. The second phase (B, Nov. 2004 – Sep. 2005) was characterized by lava filling the 3 November 2002 crater. Five lavas overflowed the summit crater into the caldera and reached lengths of a few hundred metres to about a kilometre. In addition to elevated volcano-tectonic and long period seismicity, episodes of tremor and seismic signals attributed to rockfall were detected, and seemed to be associated with the filling and then overflowing of the summit crater. In 2005, strombolian activity, pyroclastic density currents, SO_2 and ash emission accompanied lava effusion. The third phase of eruption (C, Mar – Aug 2007) was characterised by frequent, moderate explosive activity, intermittent SO_2 emission and semi-continuous effusion to both north and south of the summit crater as 3 new lava flows. The fourth phase (D, Jul 2008 – October 2009) showed an increase in the number of explosions, with some ash columns reaching 6 km height. During D, explosive activity began to build a new cone and lava dome in the summit crater. Seven new lava flows descended into the caldera, with all but one flowing to the south.

The majority of lava flows were emplaced over periods of 2–3 days. Lavas tended to follow drainage channels on the northern and southern sides of the crater, which were gradually filled during the eruption. The shape of the active cone and dome also changed dramatically.

Methods

We estimated the 2002–2009 lava volumes using two independent methods. First, we mapped individual lava flows using aerial and satellite (ASTER) imagery, and validated our remote observations during field

Table 1 Summary of monitoring data at El Reventador, 2002–2009

Method	Description and temporal coverage	Data sources
Visual observations	regular overflights and field visits; 2002–2009	Instituto Geofísico daily reports since 18/02/2003, summarised in Naranjo 2013.
Thermal camera images	Captured during 39 flights and 6 fieldwork campaigns; 2002–2009 (except 2006)	Ramón and Vallejo (2011); described in detail by Naranjo 2013.
Seismic event count	18.02.2003 – end of study period (2508 days of data)	Instituto Geofísico daily records
Satellite thermal alerts (MODVOLC, HOTSPOT)	There were 284 MODVOLC alerts at El Reventador where Bands 12 and 22 were saturated, suggesting temperature exceeding 500 K; 2002–2009	e.g., Wright et al. 2005; Naranjo 2013.
VAAC alerts	208 alerts were made about activity from El Reventador, since the onset of the eruption in 2002.	More details in Naranjo, 2013; http://www.ospo.noaa.gov/Products/atmosphere/vaac/
OMI SO_2 measurements	OMI SO_2 retrievals available since 2004. 115 images show an SO_2 plume from El Reventador	e.g., Carn et al. 2008; Naranjo 2013, http://so2.gsfc.nasa.gov/

campaigns, when we also measured lava flow thickness. These data allowed planimetric estimates of flow volume. Second, we used a small set of satellite radar interferograms ('InSAR') to derive change in topography (2000–2009) and thus a topographic estimate of lava volume.

Flow mapping from aerial and satellite imagery

Initial lava flow maps were constructed using aerial photographs to identify new lavas, and thermal images (both aerial and ground-based) to distinguish between flows of different ages and cooling histories (Vallejo and Ramón 2011). Oblique aerial photographs were captured from a height of ~1 km during aeroplane and helicopter overflights at El Reventador (see Table 1). Depending on volcanic activity and meteorological conditions, flights typically resulted in 5–10 useful photographs. An orthorectified ASTER image (e.g., Yamaguchi et al. 1998) was used in a GIS programme to identify control points, such as distinctive topographic features, in oblique aerial photographs. The boundaries of individual lava flows were then mapped and digitised at a better spatial resolution (~15 m) than had previously been possible (Vallejo 2009). Two ASTER Visible & Near Infrared images (18.11.2003 and 09.09.2010, downloaded from the AVA webpage,[2] bands 1, 2, 3 N, 3B; 0.52–0.86 μm) were also used to map lava flows in inaccessible parts of the caldera and to establish relative emplacement dates for some flows.

Field campaigns and lava thickness measurements

We checked our identification of flow boundaries during two field campaigns to the northern (June, 2012) and southern (September, 2012) parts of El Reventador caldera. During these field campaigns, we also mapped the edges of the most recent lava flows and made measurements of lava flow thicknesses (Figs. 2, 3 and 4). Where possible, lava thicknesses were measured directly at the flow fronts (Fig. 3), and several measurements were made for each flow. Thickness was measured with a tape measure and locations recorded with a handheld GPS. This was primarily at the lava flow margins on the northern and southern caldera edges where lava flows were accessible. The thickness of lava flows that were difficult to access but that could be seen clearly from a distance were determined trigonometrically from measurements collected using a laser rangefinder (LTI Truepulse, Fig. 2). Rangefinder measurements could only be made when visibility was good, but some uncertainties in thickness may still have been introduced by variations in atmospheric pressure, temperature and humidity (e.g., Petrie and Toth 2008), although these uncertainties are insignificant relative to the assumption of uniform thickness used to estimate volume (see Lava volumes and effusion rates).

Topographic change from satellite radar images

Satellite Interferometric Synthetic Aperture Radar (InSAR) allows the measurement of millimetre- to centimetre-scale

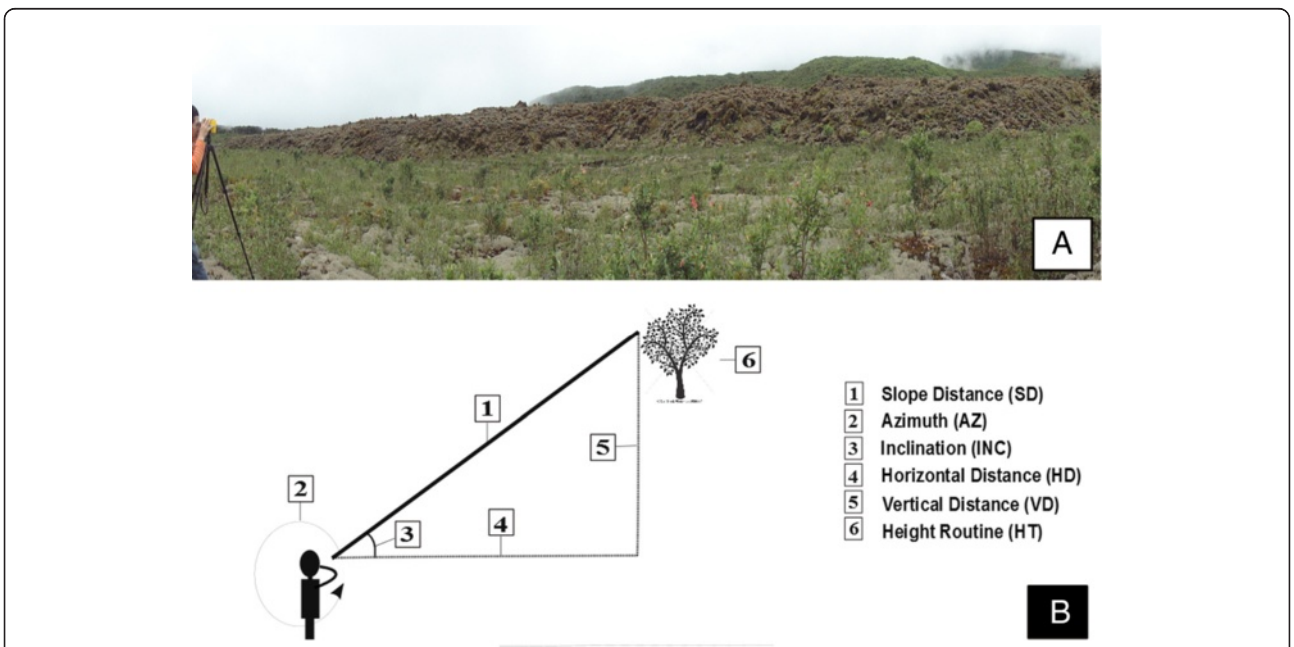

Fig. 2 a Field photograph of an EDM measurement under optimal conditions (limited cloud, good visibility, point 3 on Fig. 1). **b** Schematic drawing showing the geometry of the rangefinder used to measure lava thicknesses. Lava thicknesses were estimated as a vertical distance from the horizontal distance to the base of the flow and the direct distance to its top, using trigonometry

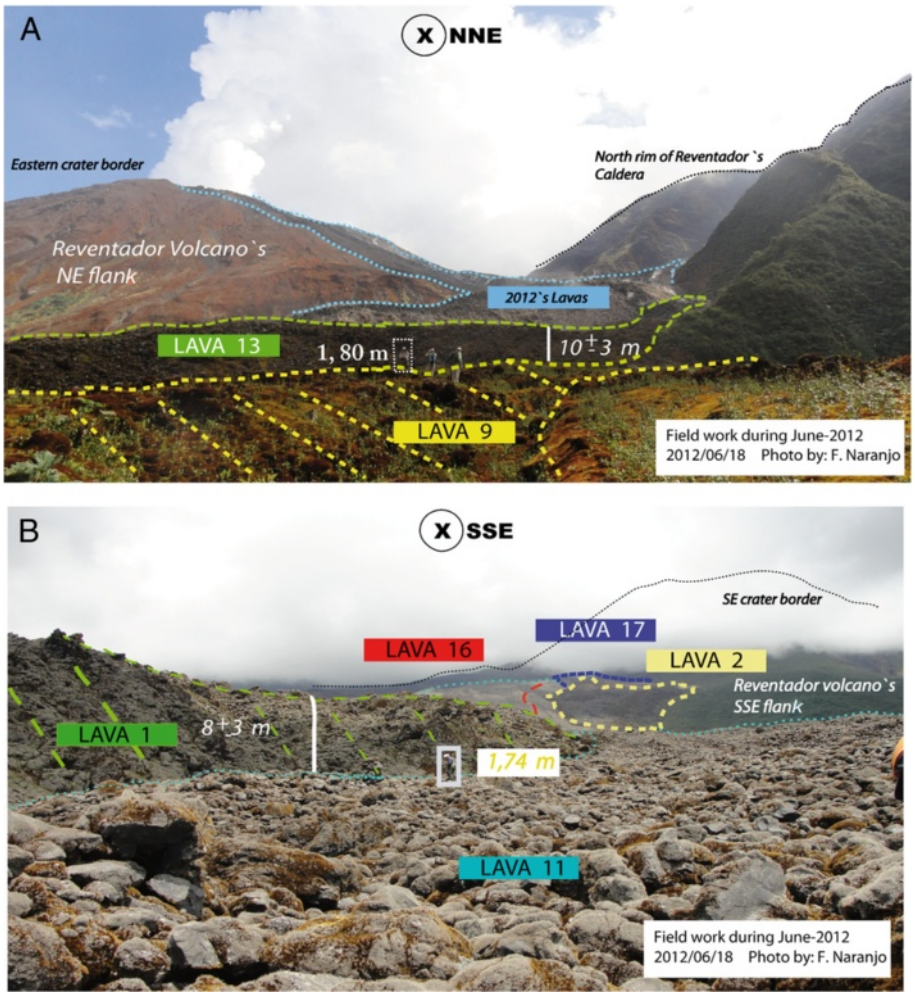

Fig. 3 a Ground photograph on north flank (point 1 in Fig. 1) showing lava flows 9 and 13 (see Table 4). **b** Ground photograph on southeastern flank (point 2 in Fig. 1) showing lava flows 1 and 11, with distant views of flows 2, 16, and 17 (see Table 4)

changes in the Earth's surface. It has been used to measure deformation at hundreds of volcanoes around the world and has captured a range of processes associated with the movement of subsurface fluids (e.g., Biggs et al. 2014; Pinel et al. 2014). Interferograms have also been used to map active lava flows (Dietterich et al. 2012), estimate topographic change (e.g., Sigmundsson et al. 1997; Wadge et al. 2006; Ebmeier et al. 2012; Poland 2014) and measure post-emplacement subsidence and mass-wasting (e.g., Stevens et al. 2001; Wadge et al. 2011; Ebmeier et al. 2014).

Interferograms are maps of the phase difference between radar images, normally used to measure displacement of the ground. However, the phase values from a set of interferograms can also be used to estimate change in topography relative to the Digital Elevation Model used in processing (e.g., Sigmundsson et al. 1997; Ebmeier et al. 2012). Change in topography since the DEM used for topographic correction was acquired (δz) can be estimated using the relationship between phase contributions from topographic change ($\delta\Phi_{topo}$) and satellite position (B_{perp}):

$$\delta z = \frac{r\lambda \sin(\nu)}{4\pi B_{perp}} \delta \varnothing_{topo},$$

where λ is radar wavelength, r is distance between satellite and the ground and υ is radar incidence angle.

We analyse seven interferograms constructed from L-band (lamba = 23 cm) SAR images acquired between 2007 and 2009 by the Japan Aerospace Exploration Agency (JAXA)'s ALOS PALSAR instrument. Interferograms were processed using JPL's ROI_PAC software (Rosen et al. 2004), and NASA's Shuttle Radar Topography Mission 30 m DEM (SRTM) was used to correct for the effect of different viewing geometries on the earth's topography (Rosen et al. 2001). If the scattering or reflecting characteristics of the earth's surface change between SAR acquisitions, then the various contributions of different

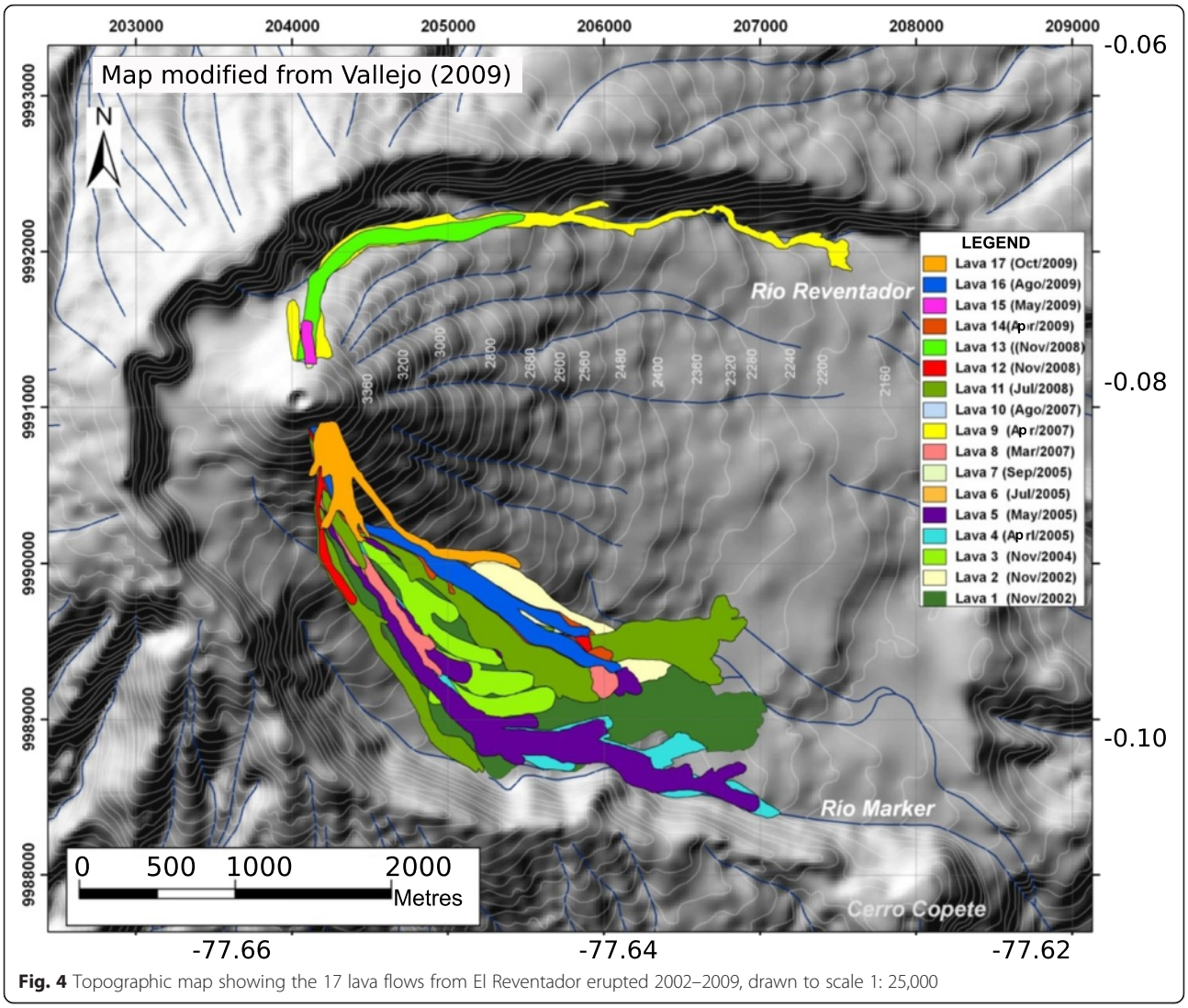

Fig. 4 Topographic map showing the 17 lava flows from El Reventador erupted 2002–2009, drawn to scale 1: 25,000

objects to the phase within a pixel will not cancel out, and data will be unusable (incoherent). Longer wavelengths penetrate further through vegetation, reducing this effect (e.g., Ebmeier et al. 2013), but at El Reventador, most of the area outside the caldera itself remains incoherent, even at L-band. The dense, rapidly changing forests around El Reventador decorrelate very quickly, so that interferograms can only be used within the caldera, where volcanic activity has produced an unvegetated surface with relatively stable scattering properties.

If we were confident that no deformation was taking place, then we could perform a single inversion to retrieve δz from phase values. However, since the lava flows at El Reventador are so young, including some that were emplaced during our period of observation, it seems likely that the interferogram phase also contains contributions from flow deformation. We therefore performed a joint inversion to retrieve both the change in height and deformation rate, assuming that deformation rate is linear.

This problem takes the form of a set of linear equations $\mathbf{d} = \mathbf{Gm}$, where $\mathbf{d}$ is a column vector with phase change for each pixel of each interferogram, $\mathbf{G}$ is a design matrix containing perpendicular baseline multiplied by a factor of $\frac{r\lambda \sin(\nu)}{4\pi}$, the time span of each interferogram and a constant. The vector $\mathbf{m}$, will therefore retrieve the best-fit change in topography (z) and best-fit linear deformation rate (k). We weight our inversion according to the estimated variance of each interferogram, and assume that any uncertainties in baseline estimation are much lower in magnitude than atmospheric contributions. Ideally, variance would be calculated using the whole interferogram to capture large-scale atmospheric features. However, as coherence is typically limited to the caldera of El Reventador itself, we use the range of phase values within the caldera (after topographic correction and avoiding areas of subsidence) as the diagonal values of a weighting matrix, $\mathbf{W}$. We neglect the effects

of co-varying atmosphere between interferograms, setting the off-diagonal elements to zero. We solve for **m** using a weighted linear least squares inversion: $\mathbf{m} = [\mathbf{G}^T\mathbf{W}_\phi^{-1}\mathbf{G}]^{-1}\mathbf{G}^T\mathbf{W}_\Phi^{-1}\mathbf{d}$, with formal errors ($\sigma_z$ and σ_k) of $[\mathbf{G}^T\mathbf{W}_\phi^{-1}\mathbf{G}]^{-1}$. We use the lower limit for topographic change ($\delta_z - \sigma_z$) as an indication of the edge of the region of topographic change and find that this matches the maps produced from field observation for most of the flow field.

Results

Lava volumes and effusion rates

We build on earlier analyses of aerial photographs, thermal imagery and field observations (Vallejo 2009; Vallejo and Ramón 2011), to identify and map 17 lava flows, erupted since 2002, at a spatial of resolution of 15 m (Fig. 4). The total surface area of each lava flow mapped was calculated from our digitised flow outlines and multiplied by a uniform thickness, which was the mean of all field thickness measurements made for that flow, to calculate an approximation of the total volume change between 2002 and 2009 (Table 2). In combination with the time over which lava flows were effused (from monitoring data, Additional file 1), this allowed the calculation of a time-averaged lava effusion rate for each individual flow, as well as for the whole period 2002–2009 (Tables 2 and 4). Our planimetric estimation of total flow volume is 90×10^6 m^3.

We estimate an uncertainty of 5 % in the lava flow surface areas derived from aerial photographs and ASTER images. Errors may be introduced by extrapolation of flow outlines where they are obscured by cloud or vegetation and by uncertainties in the location of flow edges of up to 15 m (resolution of the ASTER imagery). Uncertainties in lava thickness measurements were estimated in the field at 5–35 %, depending on measurement conditions, such as distance to lava flow, and are probably largest where measurement was prevented by deep ravines near the edges of the lava flows. We therefore expect the maximum measurement uncertainty in the volume (the sum of maximum uncertainties in lava flow areas and thicknesses) to be about 40 % (37×10^6 m^3). This may be an underestimate, because the assumption that the thickness of lava flows at their edges is the same as their interior thickness is not valid. In particular, where individual lava flows are superimposed, the resulting compound flow field is likely to have a complicated, irregular morphology. Where lavas have flowed over rough topography with varying slope, estimating mean thickness from point measurements is unlikely to be reliable.

Table 2 Comparison of time-averaged lava flow characteristics as determined from field measurements and InSAR

	Field measurement & mapping from imagery	Retrieved from radar imagery (excluding dome area)
Total surface area of flows (m^2)	$3.6 \pm 0.9 \times 10^6$	$3.4 \pm 0.7 \times 10^6$
Total lava volume (m^3)	$90 \pm 37 \times 10^6$	$75 \pm 24 \times 10^6$
Mean effusion rate (m^3/s)	9 ± 4	7 ± 2

Total volume change predicted by the InSAR inversion was treated as the sum of the area of each pixel multiplied by change in height where the topographic change retrieved exceeded the lower limit for topographic change ($\delta_z - \sigma_z$). Uncertainty in the total volume of lava flows depends on (1) how accurately the edge of the lava can be resolved and (2) the uncertainty in the thickness estimates for each pixel. We estimate that our InSAR - derived flow boundaries are within ~2 pixels (60 m) of the edges of the lava flows (e.g., Ebmeier et al. 2012). El Reventador's flow field has a perimeter of ~ 13 km, so the uncertainty in surface area is $\sim 0.7 \times 10^6$ m^2, or 18 % of the area where topographic change was detected (3.4×10^6 m^2). Within this area, lava thicknesses had an average value of ~35 m and a maximum of 55 m. Uncertainties in thickness were taken as the inversion formal errors, σ_z, and had an average value of ~5 m (14 % of average thickness). The combined uncertainty in volume change was therefore of the order of $\pm 24 \times 10^6$ m^3 (32 %) out of a total of 75×10^6 m^3. This total volume is certainly an underestimate, because the changes in scattering properties of the dome and the area immediately surrounding it meant that it was not possible to measure topographic change in this area.

Mean effusion rate between 2002 and 2009 calculated from both interferograms (7 ± 2 m^3/s) and field measurements (9 ± 4 m^3/s, Table 2) agree to within measurement uncertainty, and we expect the true rate to lie between the two values.

Development of flow field and cone

Both field measurements and InSAR retrievals agree that the thickest parts of the 2002–2009 flows are to the southeast of the active dome, where many successive lavas are superimposed. However, there is an interesting discrepancy between the two measurement methods at the thickest part of the flow: the planimetric method estimates a total of thickness 75 m, while the thickness determined from interferograms was 55 m. This is likely to be due to complicated flow morphology in this part of the flow field, where many successive lava flows of different ages have been superimposed and the assumption of individual uniform flow thickness required by the planimetric method is likely to be incorrect. Our InSAR retrievals of total topographic change 2002–2009 probably capture the shape of the total flow field more accurately

than the planimetric estimations as height is retrieved directly at a horizontal resolution of about 30 m.

The process of successive lava flows filling the crater and overflowing downslope into the caldera has been rebuilding the summit cone since 2002. Our InSAR measurements suggest that just below the summit, height increased by about 50 m between 2002 and 2009 (Fig. 5a). Some, but not all, of this height had already been rebuilt by 2004, when the summit elevation was thought to be 3355 +/− 6 m (*D. Andrade, pers. comm.*) We were not able to make radar measurements of topographic change over the dome itself, due to the rapidly changing scatterer properties during the 2007–2009 eruptions. Similarly, field measurements of dome height are not possible due to frequent explosive activity.

Post-emplacement subsidence

We perform a joint inversion to retrieve both topographic change between 2002 and 2009, and the subsidence of the lava surfaces during 2007–2009, when the SAR images were acquired. We assume that this is linear for the purposes of our inversion. Although lava deformation rate may initially decay exponentially, other studies demonstrate that by the time the surface properties of a lava have stabilised enough for an interferogram to be constructed, lava subsidence is commonly linear (e.g., examples in Table 1 in Ebmeier et al. 2012). Our maps of lava subsidence show peak displacement rate of −6 cm/year at the thickest part of the flows (Fig. 5b). In this area the total thickness of lavas emplaced 2002—2009 is ~50 m (Fig. 5a). The formal errors from our inversion of InSAR data are +/− 1.6 cm/year for a constant deformation rate, so that only subsidence at rates exceeding this value is expected to be detectible. In general, subsidence at rates greater than −1.6 cm/year is measured over the young lavas where total thickness exceeds 35 m (Fig. 5).

We do not think that the subsidence of the El Reventador lavas is related to ongoing flow processes, such as the continued flow of channelized lava (e.g., Cashman et al. 1999) or the collapse or tearing of any surface crust across the channel (e.g., Borgia et al. 1983), because such processes would cause changes to scattering properties of the surface and make interferograms incoherent. The only parts of the lava flow field that were incoherent in our measurements are those from later than July 2007, during the period when SAR images were being acquired (Lava flows 10–17 on Fig. 4).

Given that none of the lava flows measured were more than 5 years old at the time of measurement, it seems likely that the majority of the signal can be attributed to thermal contraction. However, other processes such as loss of pore space in the autobreccias may also contribute to lava flow subsidence. The subsidence of the El

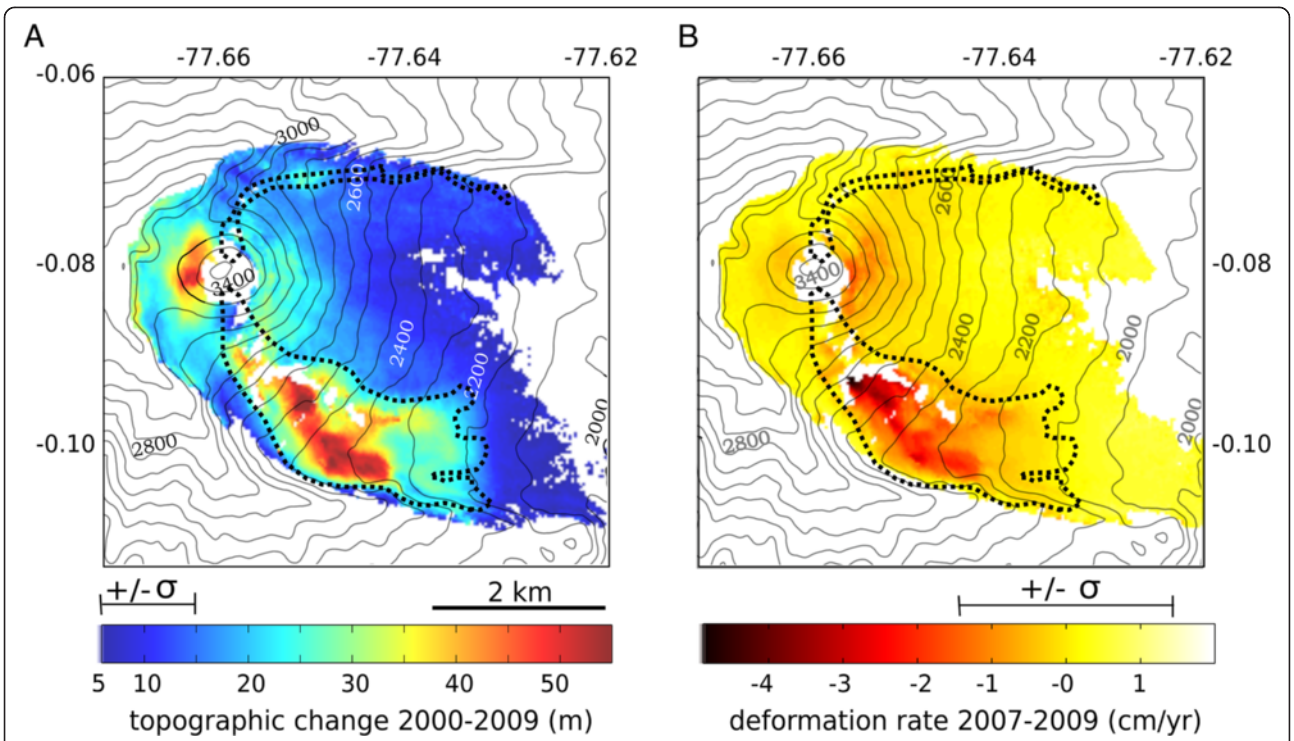

Fig. 5 a Map of topographic change retrieved from ALOS-1 interferograms (Additional file 2: Table S1). Only values that exceed our lower limit for topographic change ($\delta_z - \sigma_z$) are shown. **b** Map of lava flow subsidence at El Reventador. Displacement values are averages for a period between 2007 and 2009 when SAR images were acquired and assuming a linear deformation rate

Reventador lava flows is similar in magnitude to that measured at lava flows of similar thickness and age (e.g., Table 1 in Ebmeier et al. 2012). For example, Lu et al. (2005) measured subsidence of ~4 cm/year over 50 m thick basaltic lava flows during the fourth year after their emplacement.

Discussion

Lava flows at El Reventador in 2002–2009

Our measurement of flow volume for 2002–2009 (75×10^6 m^3, topographic estimation from InSAR) is significantly higher than that of El Reventador's last period of activity during three episodes from 1972 to 1976 (Table 3, 34.3×10^6 m^3, Hall et al. 2004). The differences in effusion rates (and duration) are matched by differences in the vigour and explosivity of the eruptions that initiated the lava effusion beginning in 1972 and 2002. While the 2002 eruption was sub-plinian (VEI 4), the 1972 event produced just moderate ash fall (VEI 3) and the eruption in 1976 was preceded by only the generation of a steam column from the crater (Hall et al. 2004). We speculate that the differences in the lava effusion rates and total erupted volume between eruptive episodes in the 1970s and 2000s (Table 3) may relate to 1) a higher rate of intrusion of primitive magma into a mid-depth reservoir in the more recent event or potentially 2) the more explosive initial eruption in 2002 clearing the vent of obstacles and establishing a wider active conduit.

The regular episodes of historical activity at El Reventador, each lasting several years, have been attributed to repeated intrusion of primitive, water-rich magmas into an andesitic magma body at 7–12 km depth (Samaniego et al. 2008). During the explosive activity of 2002, the eruption was thought to be triggered by the injection of volatile-rich basic melt from depth. Mineral assemblages and trace element ratios have been interpreted to suggest that a second intrusion of mafic magma into the reservoir took place in during 2004–2005, initiating phase B (Samaniego et al. 2008), though there is not a great change in the mineral assemblages observed in thin sections over this period. Changes in chemistry between 2004 and 2009 may be indicative of fractional crystallisation (Naranjo 2013). The bulk composition of field samples from 2007 and 2012 show a minor increase in SiO_2 content (Naranjo 2013; Table 4). Our observations of decreasing effusion rate over the course of each phase of activity may be related to increasing SiO_2 content (Table 4), and therefore increasing viscosity.

Effusion rate at El Reventador may vary in response to 1) magma supply rate (e.g., Walker 1973; Harris and Rowland 2009) and 2) melt composition, reflecting the time since last intrusion of primitive material. In the future, any reversal of the trend of decreasing flow volume and effusion rate during an eruptive phase may signal an renewed availability of magma, for example due to a new intrusion or accumulation of fluid due to magma reservoir reorganisation.

Implications for monitoring lava flows at El Reventador

The priority during eruptive phases at El Reventador has been forecasting the extent of lava flows. This is critical because of the nearby resident populations and important infrastructure (e.g., an oil pipeline). Aerial thermal imagery (and photographs in clear conditions) are more likely to be feasible during eruptions than ground-based measurements, which only become a priority outside of times of crisis. Frequent observations of lava flows

Table 3 Estimated volumes and lava effusion rates for El Reventador's two recent periods of eruption, 1972–1976, and 2002–2009

Eruptive phase	Estimated lava flow volume m^3	average effusion rate x 10^6 m^3/day
July - September 1972	10.5×10^{6a}	0.11
Nov 1973 - July 1974	3.8×10^{6a}	0.02
Jan (April) – May 1976	20.0×10^{6a}	0.13 (0.33)
Nov 2002 (phase A)	32.8×10^6	2.31
Nov 2004 – Sep 2005 (phase B)	20.1×10^6	0.53
Mar. – Sep. 2007 (phase C)	8.0×10^6	0.29
Apr. – Nov. 2009 (phase D)	26.8×10^6	0.76

Eruption period are broken down into separate phases of activity, as described in Observations of eruptions 2002–2009

[a]lava flow volumes as reported by Hall et al. 2004

Table 4 Flow parameters determined from planimetric method

Phase	Flow number	Start date dd.mm.yy	Duration (days)	Volume (x 10^6 m^3)	% SiO_2	Effusion rate (m^3/day)
A	1	09.11.02	9	26.3	56–58[a]	2.9×10^6
A	2	18.11.02	5	6.5	53–55[a]	1.3×10^6
B	3	21.11.04	8	6.6	55–56[a]	8.2×10^5
B	4	02.04.05	9	5.6	55[a]	6.3×10^5
B	5	18.05.05	10	7.2	55[a]	7.2×10^5
B	6	19.07.05	4	0.6	54[a]	1.5×10^5
B	7	14.09.05	7	0.1	–	1.8×10^4
C	8	25.03.07	11	4.6	52–53	8.7×10^5
C	9	09.04.07	9	3.2	53	
C	10	02.08.07	10	0.2	53	2.0×10^4
D	11	28.07.08	8	14.1	54	1.8×10^6
D	12	05.11.08	5	1.7	54	3.5×10^5
D	13	11.11.08	3	1.9	55	6.2×10^5
D	14	23.04.09	6	3.7	55	6.1×10^5
D	15	02.05.09	5	0.2	–	3.9×10^4
D	16	04.10.09	3	3.4	55	1.1×10^6
D	17	02.10.09	5	1.9	54	3.7×10^5

[a]SiO_2 % from Samaniego et al. 2008

during an eruptive phase are therefore challenging to obtain. However, topography during periods of quiescence is now being measured with increasing accuracy, for example using Structure from Motion methods with helicopter overflight photographs.

Conclusions

Our examination of lava flow volume and effusion rate between 2002 and 2009 at El Reventador demonstrate the strengths and weaknesses of two complementary methods for approximating lava flow volumes and thus time-averaged effusion rates. Lava volumes estimated from planimetric and satellite radar topographic approaches agree to within measurement error, although they have different systematic uncertainties. Field and aerial photographs and thermal imagery allow 17 individual lava flows to be mapped at a horizontal resolution of 15 m and variations in the effusion rate of different lava flows to be examined, assuming uniform flow thickness. In contrast, the satellite radar observations capture only the total volume change from 2002–2009, but provide a more precise measurement of flow volume because lava flow thicknesses are retrieved directly at a horizontal resolution of 30 m. Lava thickness maps derived from satellite radar are therefore useful for assessing the accuracy of higher temporal frequency planimetric methods employed during an eruption, and provide precise, additional information about lava thickness and flow field deformation. The shorter repeat measurement intervals and higher spatial resolution of current and future satellite radar instruments will make them an increasingly important tool for monitoring lava flows at remote volcanoes.

Satellite retrievals of topography, such as those presented here, have the potential to provide independent corroboration of time-averaged lava volume fluxes that rely on data from infrequent overflights or potentially dangerous ground observations. The type of measurement described here will be possible with sets of SAR images from current and future satellite missions (e.g., ALOS-2 and potentially Sentinel-1). Satellite measurement of topography is a rapidly developing field. New satellite data (especially from radar missions that acquire images designed for retrieving topography, such as TanDem-X) provide opportunities for mapping topographic change at increasingly high resolution (up to 2 × 3 m spatial resolution) and at shorter repeat times (potentially every 11 days). These improvements to spatial and temporal resolution mean that future satellite radar measurements have the potential to be a valuable supplement to ground-based monitoring, especially at inaccessible volcanoes such as El Reventador.

Endnotes

[1]1541, 1590, 1691, 1748, 1797, 1802, 1842–1843, 1944, 1856, 1871, 1894, 1898–1906, 1912, 1926, 1936, 1944, 1955, 1958, 1960, 1972, 1974, 1976, 2002- (Hall 1980; Simkin and Siebert 1994)

[2]AVA webpage http://ava.jpl.nasa.gov/ava.asp

Additional files

Additional file 1: Figure S1. Time series of monitoring parameters showing the information between 2002 and 2009. A-1: Field work in situ with direct observations of lava flows; A-2: Overflights with direct observations and thermal images; B: Thermal anomalies identified by MODIS (between the range of 330–550 °K); C: Satellite volcanic gas emission (OMI) identified with good meteorological conditions; D-1 and D-2: Ash emission associated with visual confirmation and with no visual confirmation, respectively; E: Signals associated with rock fall during the eruptive process; F: Register of explosions. Red lines correspond at the lava flows emission; periods of effusion are marked as yellow zones. (PDF 1754 kb)

Additional file 2: Table S1. Details of the ALOS PALSAR interferograms used in our analysis. (DOC 30 kb)

Competing interests

The authors declare that they have no competing interests.

Authors' contributions

Field campaigns at Reventador and analysis of monitoring data were done by MFN, SV, PR, PM and FH. Analysis of InSAR data was carried out by SKE and MFN. The manuscript was written by MFN and SKE. JB and PM first reported InSAR signals over lava flows at Reventador 2007-2010 and supported collaboration between the University of Bristol and the Instituto Geofisico. All authors read and approved the final manuscript.

Acknowledgements

We would like to acknowledge the efforts and support of Instituto Geofisico scientists and staff who have worked on monitoring El Reventador since 2002. SKE was supported by STREVA (NERC grant number: NE/J020052/1) and COMET (NERC grant number: GA/13/M/031) and is now funded by a European Space Agency Living Planet Fellowship (IMRICA). The JAXA ALOS PALSAR data presented here were provided by ASF through the WInSAR programme and have previously been described by Mothes et al. 2008.

Author details

[1]Instituto Geofísico, Escuela Politécnica Nacional, Quito, Ecuador. [2]School of Earth Sciences, University of Bristol, Bristol BS8 1RJ, UK. [3]Universidad Central del Ecuador, Quito, Ecuador.

Received: 26 September 2015 Accepted: 23 March 2016
Published online: 04 April 2016

References

Biggs J, Ebmeier SK, Aspinall W, Lu Z, Pritchard ME, Sparks RSJ, Mather TA. Global link between deformation and volcanic eruption quantified by satellite imagery. Nature Communications. 2014;5:3471. doi:10.1038/ncomms4471.

Borgia A, Linneman S, Spencer D, Morales LD, Andre JB. Dynamics of lava flow fronts, Arenal volcano, Costa Rica. J Volcanol Geothermal Res. 1983;19(3):303–29. doi:10.1016/0377-0273(83)90116-6.

Carn SA, Krueger AJ, Arellano S, Krotkov NA, Yang K. Daily monitoring of Ecuadorian volcanic degassing from space. J Volcanol Geothermal Res. 2008; 176(1):141–50. doi:10.1016/j.jvolgeores.2008.01.029.

Cashman KV, Thornber C, Kauahikaua JP. Cooling and crystallization of lava in open channels, and the transition of Pāhoehoe Lava to'A'ā. Bull Volcanol. 1999;61(5):306–23.

Cashman KV, Soule SA, Mackey BH, Deligne NI, Deardorff ND, Dietterich HR. How lava flows: new insights from applications of lidar technologies to lava flow studies. Geosphere. 2013;9(6):1664–80. doi:10.1130/GES00706.1.

Diefenbach AK, Crider JG, Schilling SP, Dzurisin D. Rapid, low-cost photogrammetry to monitor volcanic eruptions: an example from Mount St. Helens, Washington, USA. Bull Volcanol. 2012;74(2):579–87.

Dietterich HR, Poland MP, Schmidt DA, Cashman KV, Sherrod DR, Espinosa AT. Tracking lava flow emplacement on the east rift zone of Kīlauea, Hawai 'i, with synthetic aperture radar coherence. Geochem Geophys Geosyst. 2012; 13:5. doi:10.1029/2011GC004016.

Ebmeier SK, Biggs J, Mather TA, Elliott JR, Wadge G, Amelung F. Measuring large topographic change with InSAR: lava thicknesses, effusion rate and subsidence rate at Santiaguito volcano, Guatemala. Earth Planetary Sci Lett. 2012;335:216–25. doi:10.1016/j.epsl.2012.04.027.

Ebmeier SK, Biggs J, Mather TA, Amelung F. Applicability of InSAR to tropical volcanoes: insights from Central America. Geological Soc London Spec Publ. 2013;380(1):15–37. doi:10.1144/SP380.2

Ebmeier SK, Biggs J, Muller C, Avard G. Thin-skinned mass-wasting responsible for widespread deformation at Arenal volcano. Front Earth Sci. 2014;2:35. doi:10.3389/feart.2014.00035

Fink JH, Griffiths RW. Morphology, eruption rates, and rheology of lava domes; insights from laboratory models. J Geophys Res. 1998;103(B1):527–45. doi:10.1029/97JB02838.

Hall ML. El Volcanismo en E1 Ecuador. Quito: Inst. Panamer. Geogr. Histo; 1977. 120.

Hall M. El Reventador, Ecuador: un Volcán activo de los Andes Septentrionales. Revista Politécnica. 1980;5(2):123–36.

Hall M, Ramon P, Mothes P, LePennec JL, Garcia A, Samaniego P, Yepes H. Volcanic eruptions with little warning: the case of Volcán Reventador's Surprise November 3, 2002 Eruption, Ecuador. Revista geológica de Chile. 2004;31(2):349–58.

Harris A, Rowland SK. Effusion rate controls on lava flow length and the role of heat loss: a review. In: Thordarson TS, editor. Studies in Volcanology: The Legacy of George Walker. (pp. Special Publications of IAVCEI, 2, 33–51). London: Special Publications of IAVCEI; 2009. p. 2.

INECEL (Ministerio de Energía y Minas, Instituto Ecuatoriano de Electrificación). "Estudio Vulcanológico de El Reventador". Estudios realizados por INECEL y la Asociación de Firmas Consultoras del Proyecto Hidroeléctrico Coca-Codo Sinclair-Electroconsul-Tractionel-rodio-Astec – Ingeconsult – Caminos y Canales. Ambato, Ecuador: Impresión Instituto Geográfico Militar; 1988. p. 1–117

Lees JM, Johnson JB, Ruiz M, Troncoso L, Welsh M. Reventador Volcano 2005: Eruptive activity inferred from seismo-acoustic observation. J Volcanol Geothermal Res. 2008;176(1):179–90. doi:10.1016/j.jvolgeores.2007.10.006

Lu Z, Masterlark T, Dzurisin D. Interferometric synthetic aperture radar study of Okmok volcano, Alaska, 1992–2003: magma supply dynamics and postemplacement lava flow deformation. J Geophys Res (Solid Earth). 2005; 110:B02403.

Mothes P, Biggs J, Baker S, Hong S, Amelung F, Dixon T. Survey of Volcanic Activity in Ecuador using L-band SAR. AGU Fall Meeting Abstracts. 2008;1:2055.

Naranjo MF. Estudio Petro-Geoquímico y Cronológico de los Flujos de lava emitidos por el volcán Reventador entre 2002 a 2009, Proyecto de titulación previo a la obtención del título de Ingeniera Geóloga. Facultad de Geología y Petróleos. Escuela Politécnica Nacional. Repositorio de la Escuela Politécnica Nacional. 2013. Repositorio digital:bibdigital.epn.edu.ec/bitstream/15000/6443/1/CD-4972.pdf

Paz y Miño LT, y Guerrero J. La exploración al Reventador: Informe de la Comisión del Comité Nacional de Geodesia y Geofísica, compuesta por Gral. Paz y Miño, Jonás Guerrero y Cristóbal Bonifaz. Publicaciones del Ministerio de Educación Pública. pp. Imprenta Nacional. 1931

Petrie G, Toth CK. Introduction to laser ranging, profiling, and scanning, Topographic laser ranging and scanning: Principles and processing. 2008. p. 1–28.

Pinel V, Poland MP, Hooper A. Volcanology: Lessons learned from synthetic aperture radar imagery. J Volcanol Geothermal Res. 2014;289:81–113.

Poland MP. Time-averaged discharge rate of subaerial lava at Kīlauea Volcano, Hawai 'i, measured from TanDEM-X interferometry: Implications for magma supply and storage during 2011–2013. J Geophys Res. 2014;119(7):5464–81. doi:10.1002/2014JB011132

Poland MP, Miklius A, Sutton AJ, Thornber CR. A mantle-driven surge in magma supply to Kīlauea Volcano during 2003–2007. Nat Geosci. 2012;5(4):295–300. doi:10.1038/ngeo1426.

Ramón P, Vallejo S. La actividad del Volcán Reventador posterior a la gran erupción de Noviembre de 2002, Séptimas Jornadas de Ciencias de la Tierra. Quito: EPN; 2011.

Rosen PA, Hensley S, Gurrola E, Rogez F, Chan S, Martin J, Rodriguez E. SRTM C-band topographic data: quality assessments and calibration activities. In Geoscience and Remote Sensing Symposium, 2001. IGARSS'01. IEEE 2001 International. 2001;2:739–41. doi:10.1109/IGARSS.2001.976620

Rosen PA, Hensley S, Peltzer G, Simons M. Updated repeat orbit interferometry package released. Eos Trans Am Geophys Union. 2004;85(5):47. doi:10.1029/2004EO050004

Rowland SK. Slopes, lava flow volumes, and vent distributions on Volcan Fernandina, Galapagos Islands. J Geophys Res (1978–2012). 1996;101(B12): 27657-72. doi:10.1029/96JB02649

Ryan GA, Loughlin SC, James MR, Jones LD, Calder ES, Christopher T, Strutt MH, Wadge G. Growth of the lava dome and extrusion rates at Soufriere Hills Volcano Montserrat West Indies 2005–2008. Geophys Res Lett. 2010;370: L00E08. doi:10.1029/2009GL041477.

Samaniego P, Eissen JP, Le Pennec JL, Robin C, Hall ML, Mothes P, Chavrit D, Cotten J. Pre-eruptive physical conditions of El Reventador volcano (Ecuador) inferred from the petrology of the 2002 and 2004–05 eruptions. J Volcanol Geothermal Res. 2008;176(1):82–93. doi:10.1016/j.jvolgeores.2008.03.004

Sigmundsson F, Vadon H, Massonnet D. Readjustment of the Krafla spreading segment to crustal rifting measured by satellite radar interferometry. Geophys Res Lett. 1997;24(15):1843–6.

Simkin T, Siebert L. Volcanoes of the World: A Regional Directory, Gazetteer, and Chronology of Volcanism During the Last 10,000 Years. Tucson, Ariz: Geoscience; 1994. p. 349.

Stasiuk MV, Jaupart C, Sparks RSJ. On the variations of flow rate in non-explosive lava eruptions. Earth Planetary Sci Lett. 1993;114(4):505–16. doi:10.1016/0012-821X(93)90079-O

Stevens NF, Wadge G, Murray JB. Lava flow volume and morphology from digitised contour maps: a case study at Mount Etna, Sicily. Geomorphology. 1999;28(3–4):251–61. doi:10.1016/S0169-555X(98)00115-9.

Stevens NF, Wadge G, Williams CA, Morley JG, Muller JP, Murray JB, Upton M. Surface movements of emplaced lava flows measured by synthetic aperture radar interferometry. J Geophys Res (1978–2012). 2001;106(B6):11293–313. doi:10.1029/2000JB900425

Vallejo S. Identificación de límites de flujos de lava en el Volcán Reventador en base a imágenes térmicas desde el 2002. Quito: IG EPN; 2009.

Vallejo S, Ramón P. Evolución del cono de escoria y domo al interior del Cráter del Volcán Reventador 2010–2011. Jornadas de Ciencias de la Tierra y I Encuentro sobre Riesgos y Desastres, 179–182. 2011.

Vallejo S, Ramón P. Growth And Evolution Of A Scoria Cone And Dome Inside The Reventador Volcano Crater.2010-2011, Cities on Volcanoes 7, Colima, México. 2012

Wadge G, Dorta DO, Cole PD. The magma budget of Volcán Arenal, Costa Rica from 1980 to 2004. J Volcanol Geothermal Res. 2006;157(1):60–74. doi:10.1016/j.jvolgeores.2006.03.037

Wadge G, Cole P, Stinton A, Komorowski JC, Stewart R, Toombs AC, Legendre Y. Rapid topographic change measured by high-resolution satellite radar at Soufriere Hills Volcano, Montserrat, 2008–2010. J Volcanol Geothermal Res. 2011;199(1):142–52. doi:10.1016/j.jvolgeores.2010.10.011

Walker G. Lengths of lava flows. Phil Trans R Soc Lond A. 1973;274:107–18.

Wright R, Carn SA, Flynn LP. A satellite chronology of the May–June 2003 eruption of Anatahan volcano. J Volcanol Geothermal Res. 2005;146(1):102–16. doi:10.1016/j.jvolgeores.2004.10.021

Xu W, Jónsson S. The 2007–8 volcanic eruption on Jebel at Tair island (Red Sea) observed by satellite radar and optical images. Bull Volcanol. 2014;76(2):1–14. doi:10.1007/s00445-014-0795-9

Yamaguchi Y, Kahle AB, Tsu H, Kawakami T, Pniel M. Overview of advanced spaceborne thermal emission and reflection radiometer (ASTER). Geoscience Remote Sensing IEEE Trans. 1998;36(4):1062–71.